

Supplementary Online Content

Maharaj A, Wu H, Hornik CP, et al; for the Best Pharmaceuticals for Children Act–Pediatric Trials Network Steering Committee. Simulated assessment of pharmacokinetically guided dosing for investigational treatments of pediatric patients with coronavirus disease 2019. *JAMA Pediatr*. Published online June 5, 2020. doi:10.1001/jamapediatrics.2020.2422

eMethods. Adult PBPK Model Evaluation

eTable 1. Hydroxychloroquine adult PBPK model parameterization

eTable 2. Adult PBPK Model Evaluation

eTable 3. Average Unbound Hydroxychloroquine Concentrations (C_{avg}) in Plasma Over 120 Hours in Children and Adults Using the Proposed Dosing Scheme*

eTable 4. Simulated Remdesivir Plasma Exposures (AUC from time 0 to ∞) Following Loading Dose Administration in Children and Adults under the Proposed Dosing Algorithm (Day 1)*

eTable 5. Simulated remdesivir plasma exposures (area under the concentration time curve [AUC] from time 0 to ∞) following loading dose administration in children and adults based on dosages recommended for Ebola virus disease

eTable 6. Average unbound hydroxychloroquine concentrations (C_{avg}) in plasma over 120 hours in children and adults using the proposed dosing scheme. Simulations computed using an alternative PBPK model that assumed proportional contributions of CYP2C8, CYP2D6 and CYP3A4 to hepatic intrinsic clearance were 59%, 16%, and 25%, respectively, based on in-vitro chloroquine metabolism data¹⁷

eFigure 1. Evaluation of the Developed Adult PBPK Model in Whole Blood and Plasma

eFigure 2. Comparison of Plasma Unbound Hydroxychloroquine Concentrations

eFigure 3. Comparison of Unbound Hydroxychloroquine Concentrations in Plasma to Lung Interstitial Fluid in Adults and Different Pediatric Age Groups

eFigure 4. Simulated Plasma Exposures for Remdesivir

eFigure 5. Comparison Simulated Hydroxychloroquine Concentrations in (A) Plasma/Serum and (B) Unbound Plasma/Serum Between Published Adult Models

eFigure 6. Comparison of Mean Plasma Remdesivir Exposures Versus Dose in Healthy Adult Volunteers

eFigure 7. Mean GS441524 Peripheral Blood Mononuclear Cell Exposures Versus Mean Plasma Remdesivir Exposures

This supplementary material has been provided by the authors to give readers additional information about their work.

eMethods. Adult PBPK Model Evaluation

The developed adult PBPK model was evaluated against PK data from 3 studies not used for model development.^{1–3} All studies investigated hydroxychloroquine disposition in whole blood or plasma following oral administration of the drug as its sulfate salt (200 mg of hydroxychloroquine sulfate = 155 mg hydroxychloroquine base). Studies used for model evaluation included both healthy volunteers and subjects with rheumatoid arthritis. For each study, 100 virtual subjects were generated using PK-Sim's® population algorithm based on the demographics observed in subjects (age, weight, and sex).⁴ Population-PBPK simulations were created using each virtual population in conjunction with study-specific parameters (e.g., dose, sampling matrix [blood vs. plasma], and sampling time). Two approaches were used to evaluate model predictions: (1) a visual predictive check, where PBPK model predictions were compared to estimates derived from empirically-based PK models, fit to blood and plasma concentration-time data from 5 healthy adult subjects³; and (2) a quantitative comparison of PK parameters, including maximum concentration (C_{max}) and area of the concentration time curve (AUC_{0-t}), between PBPK model predictions and observed data. Ratios comparing the average PBPK model predicted vs. observed values were generated.

eTable 1. Hydroxychloroquine adult PBPK model parameterization

Parameter	Input Value	Reference
Physicochemical properties		
Molecular weight (g/mol)	335.87	5
Log <i>P</i>	3.53	6-8,*
pKa	8.27 (base) 9.67 (base)	5
Absorption, distribution, metabolism, and excretion properties		
Blood-to-plasma partition ratio	5.4	3,8,9
Fraction unbound plasma	0.48	10
Plasma protein binding partner	α1-acid glycoprotein	11,12
Solubility of hydroxychloroquine sulfate (phosphate-buffered saline)	5 mg/mL (at pH 7.2)	13,a
Formulation dissolution	T _{50%} =0.28h (Weibull function; shape factor 0.92)	2,a
Intestinal permeability	1.06 x 10 ⁻⁵ cm/min	6-8,*a,b
Hepatic intrinsic clearance CYP2C8	0.195 mL/min (per mL of hepatic tissue)	6-8,*b
Hepatic intrinsic clearance CYP2D6	0.191 mL/min (per mL of hepatic tissue)	6-8,*b
Hepatic intrinsic clearance CYP3A4	0.048 mL/min (per mL of hepatic tissue)	6-8,*b
Glomerular filtration rate fraction	1	
Tubular secretion intrinsic clearance (Multi-antimicrobial extrusion protein-1)	0.486 mL/min (per mL of kidney tissue)	3,8,*c
Tissue:plasma partition coefficients	PK-Sim® standard algorithm	
Cellular permeability	PK-Sim® standard algorithm	
<p>*optimized based on blood or plasma concentration-time data from human in-vivo studies</p> <p>^ahydroxychloroquine is classified as Biopharmaceutics Classification System class 1 drug (high solubility, high permeability).¹⁴ As such, age-specific changes in gastrointestinal physiology and use of alternative formulations (i.e., tablet vs. extemporaneously prepared suspension) were not anticipated to influence bioavailability. Consequently, adult model parameters associated with oral absorption (e.g., intestinal permeability, dissolution time, gastrointestinal solubility) were maintained for pediatric simulations</p> <p>^bcontributions of each hepatic isozyme were defined based in-vitro drug metabolism data for chloroquine using human liver microsomes and recombinant cytochrome P450 enzymes.¹⁵</p> <p>^crenal tubular secretion was optimized assuming 26% of the administered intravenous dose appears in the urine unchanged. Transport was assumed to be facilitated by multi-antimicrobial extrusion protein-1 based on in-vitro transporter data for chloroquine.¹⁶</p> <p>log <i>P</i> indicates logarithm of the octanol-water partition coefficient; pKa, negative logarithm of the acid dissociation constant; PBPK, physiologically-based pharmacokinetic; and T_{50%}, time until 50% of the formulation is dissolved.</p>		

eTable 2. Adult PBPK Model Evaluation

Matrix	Dose ^a [mg]	Route (formulation)	C _{max} (obs) ^b [ng/mL]	C _{max} (pred) ^b [ng/mL]	C _{max} ratio (pred/obs)	AUC _{100h} (obs) [ng*h/mL]	AUC _{100h} (pred) ^b [ng*h/mL]	AUC _{100h} ratio (pred/obs)	Reference
Plasma	200	Oral (tablet)	46	41	0.89	5802 ^c	5979	1.03	3
Blood	200	Oral (tablet)	244	236	0.96	898 ^c	1052	1.17	3
Blood	200	Oral (tablet)	221	179	0.81	X	x	x	1
Blood	200	Oral (tablet)	214	191	0.89	X	x	x	2

^aDose expressed as hydroxychloroquine sulfate

^bArithmetic average based on observed data or population-PBPK simulations

^cEstimated based on an empirically-based PK model, generated from 5 healthy adult subjects receiving a single 200 mg dose (tablet) of hydroxychloroquine sulfate

AUC_{100h} indicates area under the concentration time curve over 100 hours; C_{max}, maximum concentration; obs, observed; pred, predicted; PBPK, physiologically-based pharmacokinetic

eTable 3. Average Unbound Hydroxychloroquine Concentrations (C_{avg}) in Plasma Over 120 Hours in Children and Adults Using the Proposed Dosing Scheme*

Age-group	Geometric Mean (CV% ^a) [ng/mL]	Median (IQR ^b) [ng/mL]
Neonate (0–<30 days)	35 (12)	36 (4.9)
Young infant (1–<6 months)	32 (15.1)	33 (6.4)
Infant (6–<24 months)	34 (15.6)	34 (7.1)
Young child (2–<6 years)	33 (14)	33 (6.7)
Child (6–<12 years)	34 (15.6)	33 (6.7)
Adolescent (12–18 years)	34 (23.5)	36 (11.4)
Adult (20–50 years)	32 (29.2)	32 (12.8)

^aCV, coefficient of variation
^bIQR, interquartile range
*Values computed over 600 virtual pediatric subjects, ranging from 0 to 18 years postnatal age, and 500 virtual adult subjects

eTable 4. Simulated Remdesivir Plasma Exposures (AUC from time 0 to ∞) Following Loading Dose Administration in Children and Adults under the Proposed Dosing Algorithm (Day 1)*

Age-group	Geometric Mean (CV%^a) [ng*h/mL]	Median (IQR^b) [ng*h/mL]
Neonate (0–<30 days)	4511 (29.6)	4467 (1777.5)
Young infant (1–<6 months)	4399 (33.5)	4347 (2006)
Infant (6–<24 months)	5027 (31.0)	5034 (1950.4)
Young child (2–<6 years)	4638 (31.7)	4666 (1981.8)
Child (6–<12 years)	4315 (30.6)	4299 (1634.9)
Adolescent (12–18 years)	4524 (32.9)	4465 (2051.5)
Adult (20–50 years)	4398 (35.3)	4330 (2148.7)

^aCV, coefficient of variation
^bIQR, interquartile range
*Values computed over 6000 virtual pediatric subjects, ranging from 0 to 18 years postnatal age, and 1000 virtual adult subjects
AUC indicates area under the plasma concentration-time curve

eTable 5. Simulated remdesivir plasma exposures (area under the concentration time curve [AUC] from time 0 to ∞) following loading dose administration in children and adults based on dosages recommended for Ebola virus disease^a

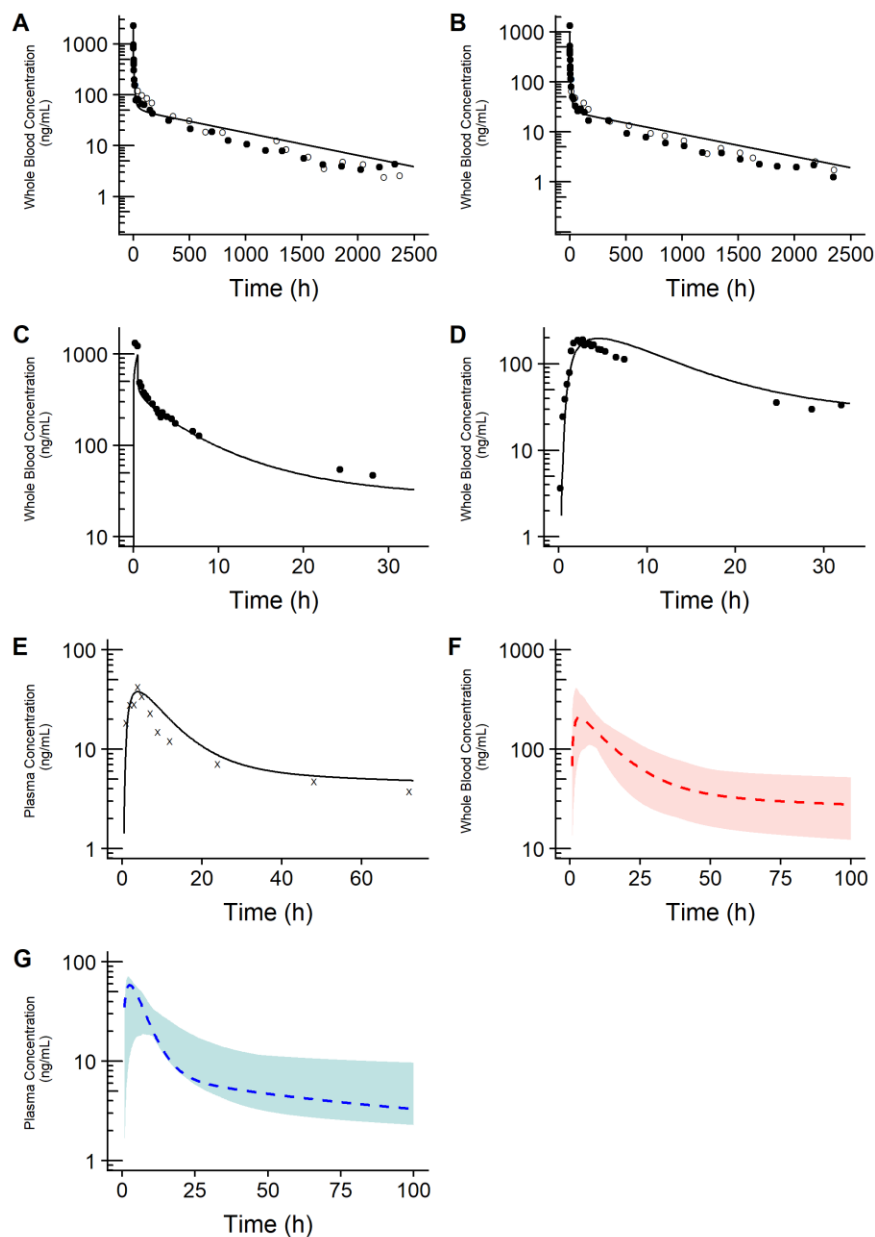
Age-group	Geometric Mean (CV%^b) [ng*h/mL]	Median (IQR^c) [ng*h/mL]
Neonate (0 - <30 days)	11264 (29.4)	11169 (4443.7)
Young infant (1 - <6 months)	10373 (32.1)	10409 (4810.9)
Infant (6 - <24 months)	8341 (30.1)	8363 (3201.5)
Young child (2 - <6 years)	6959 (30.8)	6993 (2838.8)
Child (6 - <12 years)	6454 (30.6)	6416 (2489.3)
Adolescent (12 - 18 years)	5158 (36.4)	5108 (2665.2)
Adult (20 - 50 years)	4398 (35.3)	4330 (2148.7)
^a Adults (200 mg IV); Children (200 mg IV for ≥ 40 kg or 5 mg/kg IV for <40 kg) ^b CV, coefficient of variation ^c IQR, interquartile range *Values computed over 6000 virtual pediatric subjects, ranging from 0 to 18 years postnatal age, and 1000 virtual adult subjects		

eTable 6. Average unbound hydroxychloroquine concentrations (C_{avg}) in plasma over 120 hours in children and adults using the proposed dosing scheme. Simulations computed using an alternative PBPK model that assumed proportional contributions of CYP2C8, CYP2D6 and CYP3A4 to hepatic intrinsic clearance were 59%, 16%, and 25%, respectively, based on in-vitro chloroquine metabolism data¹⁷

Age-group	Geometric Mean (CV%^a) [ng/mL]	Median (IQR^b) [ng/mL]
Neonate (0 - <30 days)	36 (9.6)	36 (5.1)
Young infant (1 - <6 months)	34 (13.4)	34 (5.7)
Infant (6 - <24 months)	34 (14.6)	34 (6.4)
Young child (2 - <6 years)	33 (12.6)	34 (6.3)
Child (6 - <12 years)	34 (14.8)	34 (6.6)
Adolescent (12 - 18 years)	35 (23.8)	37 (12.1)
Adult (20 - 50 years)	32 (28.6)	32 (12.1)
^a CV, coefficient of variation ^b IQR, interquartile range *Values computed over 600 virtual pediatric subjects, ranging from 0 to 18 years postnatal age, and 500 virtual adult subjects		

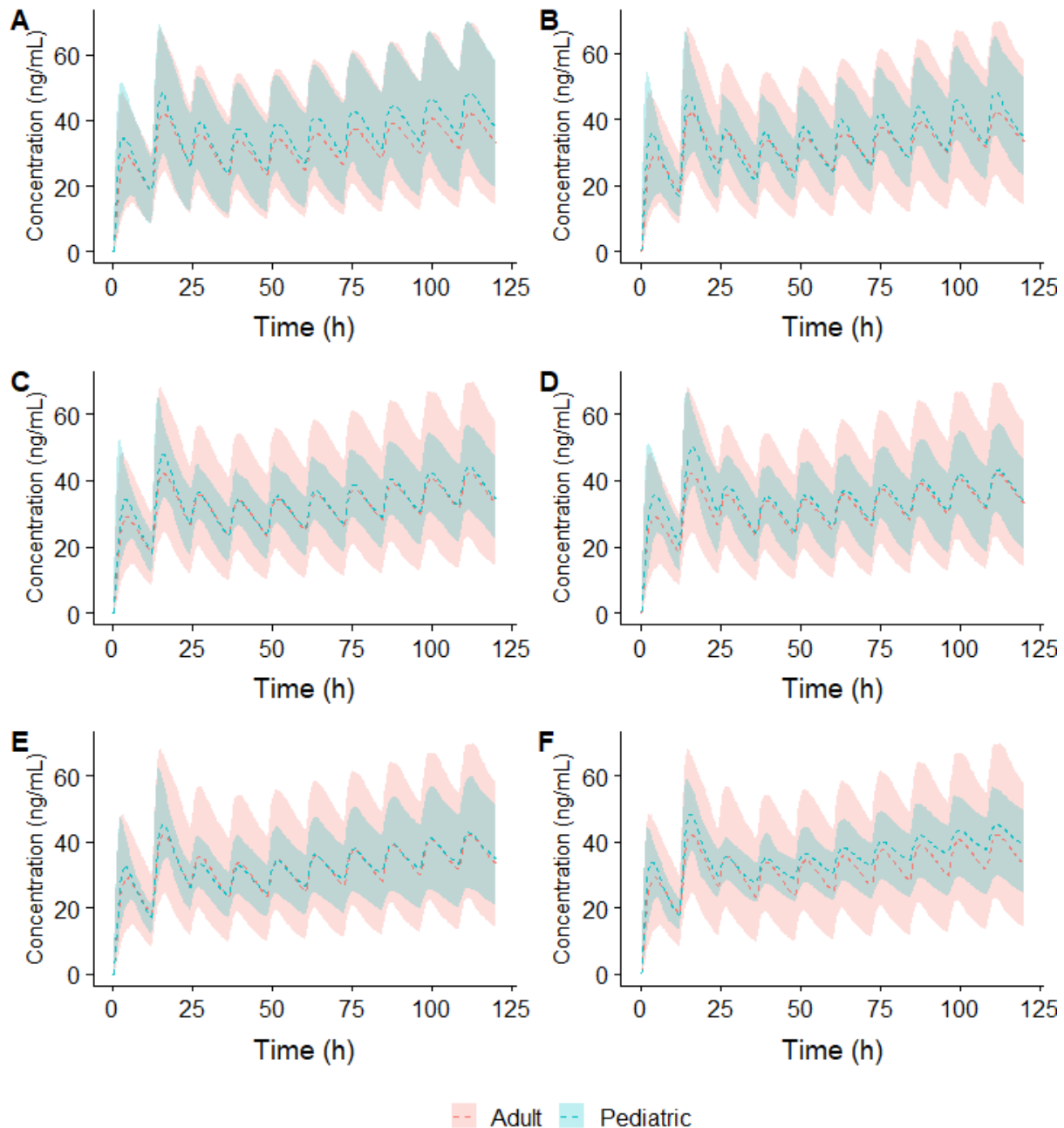
eFigure 1. Evaluation of the Developed Adult Hydroxychloroquine PBPK Model in Whole Blood and Plasma

Comparison of simulated hydroxychloroquine concentrations (whole blood and plasma) from the developed adult PBPK model against literature-based (i.e., observed) data. Studies used for optimization of the adult PBPK model are depicted in subplots A-E.⁶⁻⁸ Subplots F and G, depict an external evaluation of model simulations against estimates from an empirically-based PK model.³ Each subplot depicts single-dose administration. In subplots A-E, the solid line depicts simulated concentrations for a typical individual based on the participant demographics from each respective study; solid and open circles represent digitized concentrations for individual study participants; and X represent digitized arithmetic mean concentrations among study participants. In subplots F and G, PBPK model-derived 95% prediction intervals, generated using 100 virtual adult subjects, are depicted by colored regions. Whole-blood and plasma concentration estimates from the empirically-based PK model, generated from 5 healthy adult subjects, are displayed by dashed lines.³ Dosage and the route of administration for each assessment were as follows (expressed as hydroxychloroquine sulfate): A, 400 mg intravenous⁸; B, 200 mg intravenous⁸; C, 200 mg intravenous⁷; D, 200 mg oral tablet⁷; E, 200 mg oral tablet⁶; F, 200 mg oral tablet³; and G, 200 mg oral tablet³. Depicted arithmetic mean concentrations expressed in subplot E were representative of the test formulation and are based on a cohort of 20 male participants.⁶ Data were extracted from published figures using a plot digitizer (Graph Grabber v2, Quintessa Limited, Henley-on-Thames, UK).



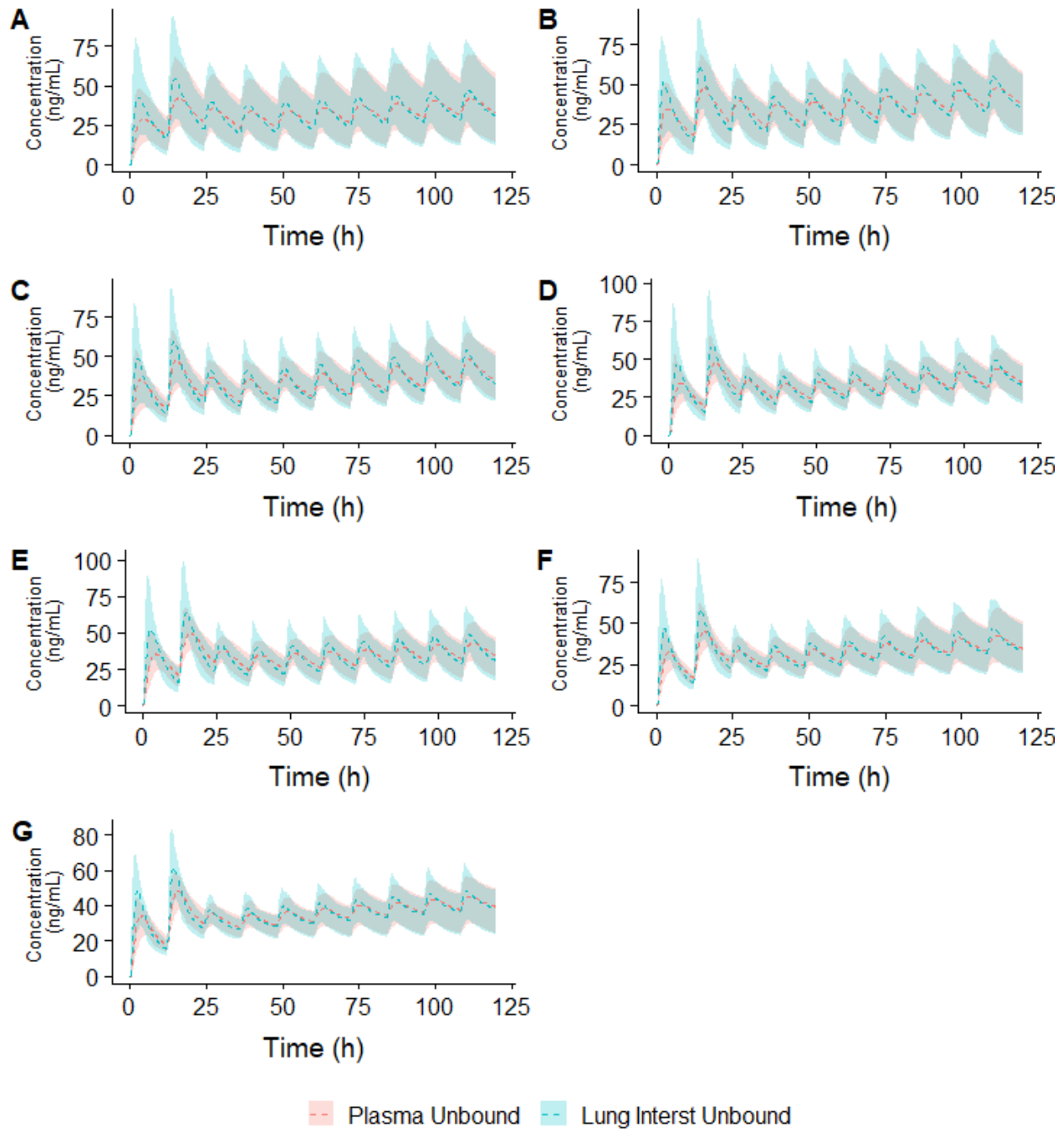
eFigure 2. Comparison of Plasma Unbound Hydroxychloroquine Concentrations

Comparison of plasma unbound hydroxychloroquine concentrations between different pediatric age groups and adults under the proposed dosing algorithm. Model generated median and 95% prediction intervals are displayed as dashed lines and colored areas, respectively. Subplots compare hydroxychloroquine concentrations between adults and different pediatric age groups, including adolescents (12-18 years, A), children (6-<12 years, B), young children (2-<6 years, C), infants (6-<24 months, D), young infants (1-<6 months, E), and neonates (0-<30 days, F).



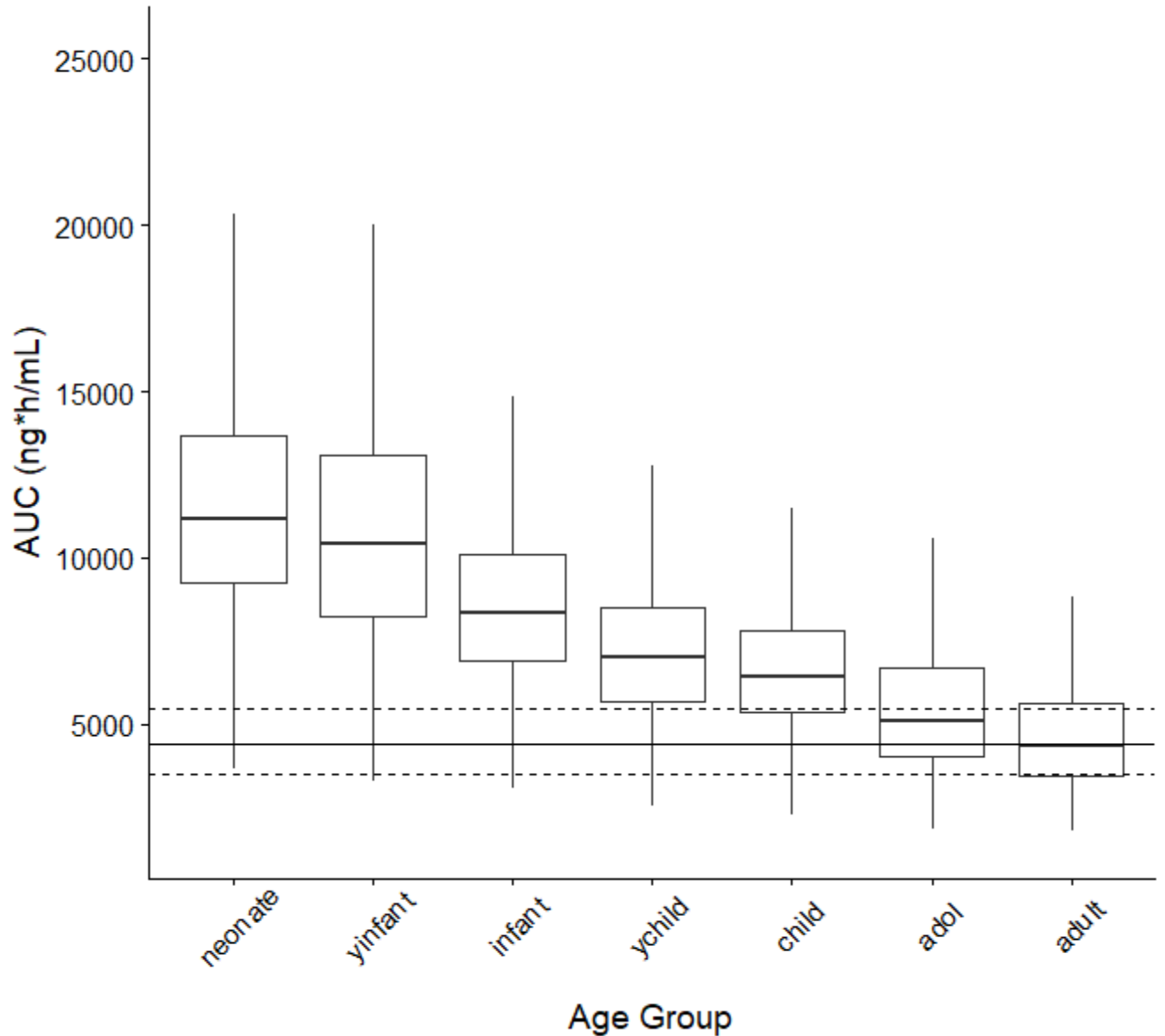
eFigure 3. Comparison of Unbound Hydroxychloroquine Concentrations in Plasma to Lung Interstitial Fluid in Adults and Different Pediatric Age Groups

Comparison of unbound hydroxychloroquine concentrations in plasma to lung interstitial fluid in adults and different pediatric age groups under the proposed dosing algorithm. Model generated median and 95% prediction intervals are displayed as dashed lines and colored areas, respectively. Subplots depict disposition in adults (20–50 years, A), adolescents (12–18 years, B), children (6–<12 years, C), young children (2–<6 years, D), infants (6–<24 months, E), young infants (1–<6 months, F), and neonates (0–<30 days, G).



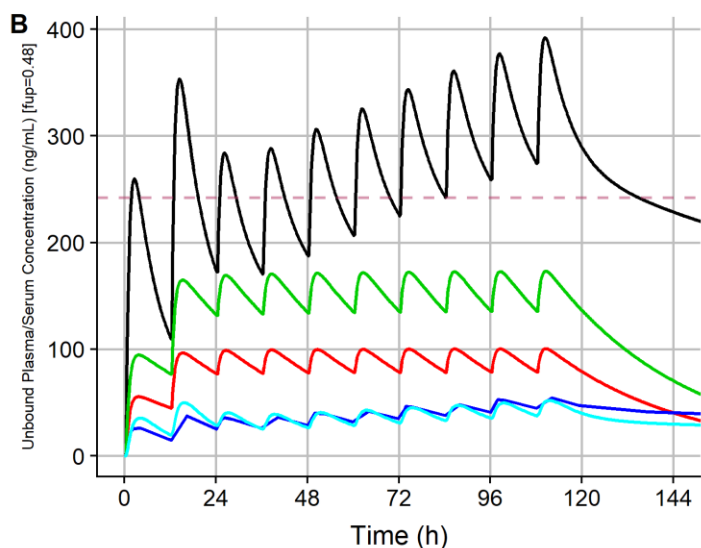
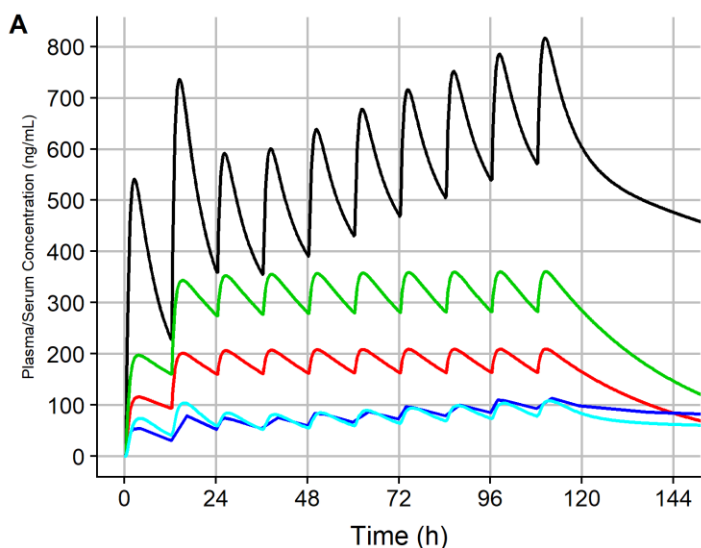
eFigure 4. Simulated Plasma Exposures for Remdesivir

Simulated plasma exposures for remdesivir (area under the concentration time curve [AUC] from time 0 to ∞) in children and adults under proposed dosages for treatment of Ebola virus disease. Exposures representative of loading dose administration [see Supplementary Table S2 footnote]. Age classifications are based on postnatal age and are defined as follows: neonate (0-<30 days), young infant (yinfant, 1-<6 months), infant (6-<24 months), young child (ychild, 2-<6 years), child (6-<12 years), adolescent (adol, 12-18 years), and adult (20-50 years).



eFigure 5. Comparison Simulated Hydroxychloroquine Concentrations in (A) Plasma/Serum and (B) Unbound Plasma/Serum Between Published Adult Models

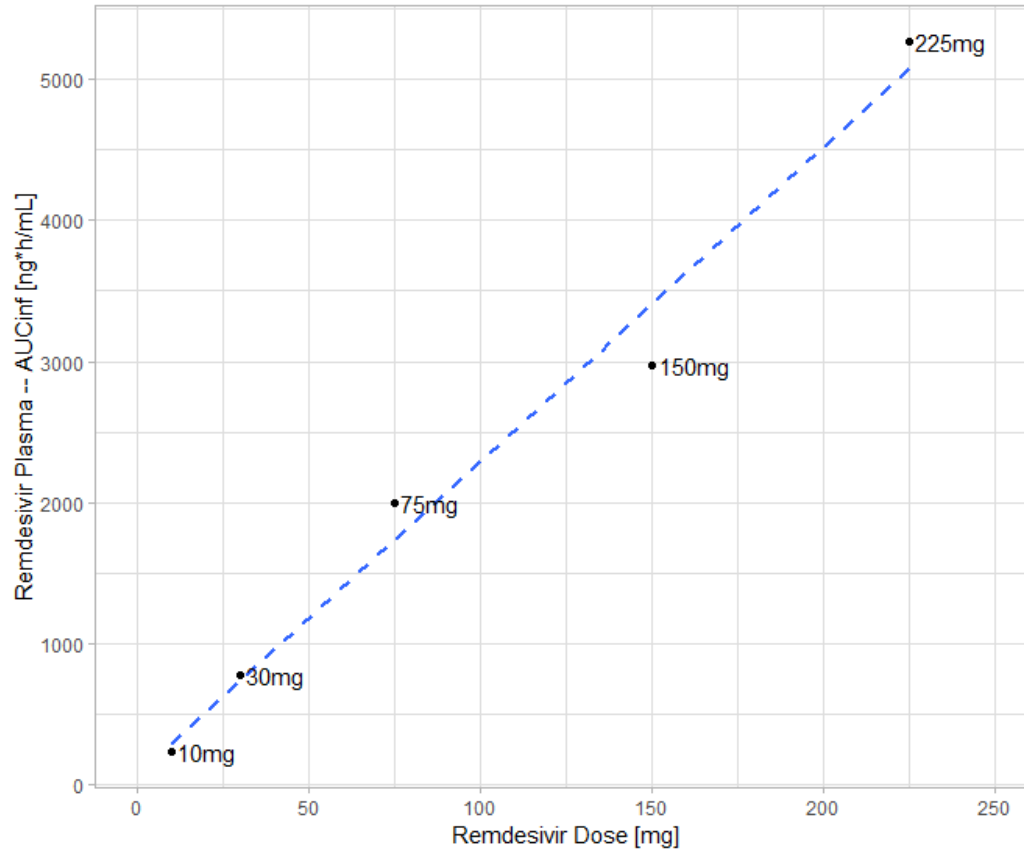
Comparison simulated hydroxychloroquine concentrations in (A) plasma/serum and (B) unbound plasma/serum between published adult models.^{9,18–20} Population pharmacokinetic (PopPK) simulations for a typical adult individual were based on parameters defined in each publication. Physiologically-based pharmacokinetic model (PBPK) simulations from the current model were based on a 70 kg adult subject (white, male). All models simulated a dosage regimen consisting of hydroxychloroquine sulfate 400 mg q12h x 2 doses followed by 200 mg q12h x 8 doses. Unbound plasma/serum concentrations were estimated from plasma/serum assuming a fraction unbound (fup) of 0.48. A reference line reflective an in-vitro determined effective concentration 50% value for hydroxychloroquine is depicted in subplot B (0.72 uM, 242 ng/mL).²⁰ Simulations corresponding to Yao et al.'s PBPK model were digitized from their published manuscript using a plot digitizer (Graph Grabber v2, Quintessa Limited, Henley-on-Thames, UK).²⁰ All PopPK model simulations were performed in R (version 3.4.3, R Foundation for Statistical Computing, Vienna, Austria) and RStudio (version 1.1.383, RStudio, Boston, MA, USA) with the RxODE package.²¹



— Lim et al [PopPK]
 — Morita et al. [PopPK]
 — Balevic et al. [PopPK]
 — Yao et al. [PBPK]
 — Current Study [PBPK]

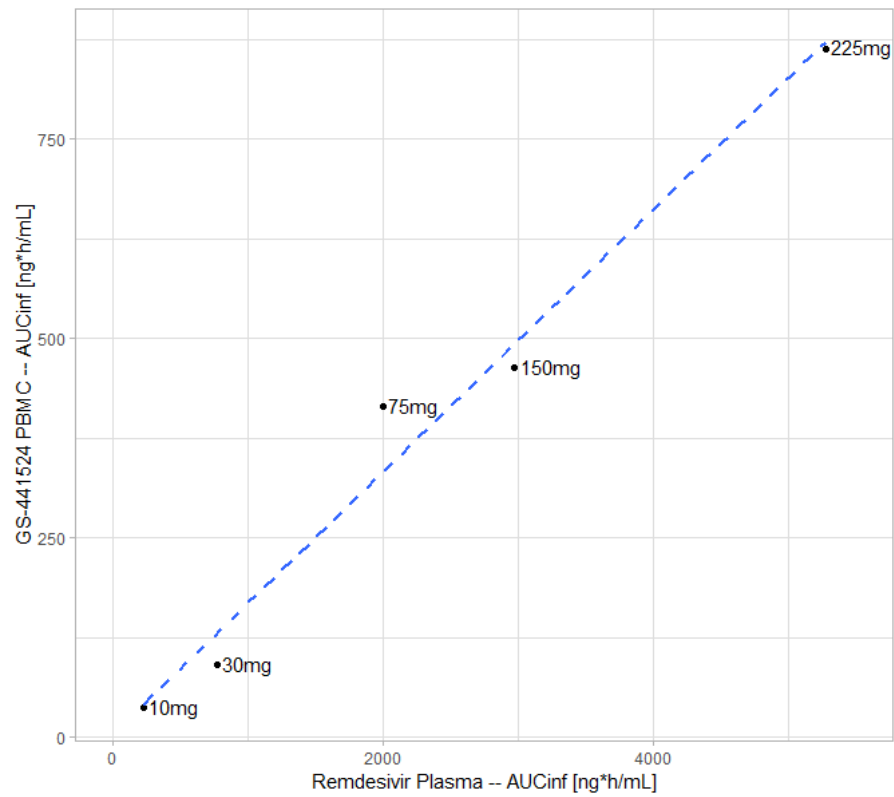
eFigure 6. Comparison of Mean Plasma Remdesivir Exposures Versus Dose in Healthy Adult Volunteers

Comparison of mean plasma remdesivir exposures (AUC_{inf}) versus dose in healthy adult volunteers (Study: GS-US-399-1812).²² Line of best fit (linear regression) is displayed for reference. Remdesivir dose (mg) is annotated.



eFigure 7. Mean GS441524 Peripheral Blood Mononuclear Cell Exposures Versus Mean Plasma Remdesivir Exposures

Comparison of mean GS441524 peripheral blood mononuclear cell exposures versus mean plasma remdesivir exposures (AUC_{inf}) healthy adult volunteers (Study: GS-US-399-1812).²² Line of best fit (linear regression) is displayed for reference. Remdesivir dose (mg) is annotated.



Supplemental References

1. McLachlan AJ, Tett SE, Cutler DJ, Day RO. Bioavailability of hydroxychloroquine tablets in patients with rheumatoid arthritis. *Br J Rheumatol*. 1994;33(3):235–239.
2. McLachlan AJ, Tett SE, Cutler DJ, Day RO. Absorption and in vivo dissolution of hydroxychloroquine in fed subjects assessed using deconvolution techniques. *Br J Clin Pharmacol*. 1993;36(5):405–411.
3. Tett SE, Cutler DJ, Day RO, Brown KF. Bioavailability of hydroxychloroquine tablets in healthy volunteers. *Br J Clin Pharmacol*. 1989;27(6):771–779.
4. Willmann S, Hohn K, Edginton A, et al. Development of a physiology-based whole-body population model for assessing the influence of individual variability on the pharmacokinetics of drugs. *J Pharmacokinet Pharmacodyn*. 2007;34(3):401–431.
5. Wishart DS, Feunang YD, Guo AC, et al. DrugBank 5.0: a major update to the DrugBank database for 2018. *Nucleic Acids Res*. 2018;46(D1):D1074–D1082.
6. Fan HW, Ma ZX, Chen J, Yang XY, Cheng JL, Li YB. Pharmacokinetics and bioequivalence study of hydroxychloroquine sulfate tablets in Chinese healthy volunteers by LC-MS/MS. *Rheumatol Ther*. 2015;2(2):183–195.
7. Tett SE, Cutler DJ, Day RO. Bioavailability of hydroxychloroquine tablets assessed with deconvolution techniques. *J Pharm Sci*. 1992;81(2):155–159.
8. Tett SE, Cutler DJ, Day RO, Brown KF. A dose-ranging study of the pharmacokinetics of hydroxy-chloroquine following intravenous administration to healthy volunteers. *Br J Clin Pharmacol*. 1988;26(3):303–313.
9. Morita S, Takahashi T, Yoshida Y, Yokota N. Population pharmacokinetics of hydroxychloroquine in Japanese patients with cutaneous or systemic lupus erythematosus. *Ther Drug Monit*. 2016;38(2):259–267.
10. McLachlan AJ, Cutler DJ, Tett SE. Plasma protein binding of the enantiomers of hydroxychloroquine and metabolites. *Eur J Clin Pharmacol*. 1993;44(5):481–484.
11. Brocks DR, Skeith KJ, Johnston C, et al. Hematologic disposition of hydroxychloroquine enantiomers. *J Clin Pharmacol*. 1994;34(11):1088–1097.
12. Furst DE. Pharmacokinetics of hydroxychloroquine and chloroquine during treatment of rheumatic diseases. *Lupus*. 1996;5 Suppl 1:S11–15.
13. Cayman Chemical. Safety data sheet: hydroxychloroquine (sulfate). Cayman Chemical web site. <https://www.caymanchem.com/msdss/17911m.pdf>. Updated November 11, 2018. Accessed April 15, 2020.
14. Pauli E, Joshi H, Vasavada A, Brackett J, Towa L. Evaluation of an immediate-release formulation of hydroxychloroquine sulfate with an interwoven pediatric taste-masking system. *J Pharm Sci*. 2020;109(4):1493–1497.
15. Li XQ, Bjorkman A, Andersson TB, Gustafsson LL, Masimirembwa CM. Identification of human cytochrome P(450)s that metabolise anti-parasitic drugs and predictions of in vivo drug hepatic clearance from in vitro data. *Eur J Clin Pharmacol*. 2003;59(5–6):429–442.
16. Muller F, Konig J, Glaeser H, et al. Molecular mechanism of renal tubular secretion of the antimalarial drug chloroquine. *Antimicrob Agents Chemother*. 2011;55(7):3091–3098.
17. Projean D, Baune B, Farinotti R, et al. In vitro metabolism of chloroquine: identification of CYP2C8, CYP3A4, and CYP2D6 as the main isoforms catalyzing N-desethylchloroquine formation. *Drug Metab Dispos*. 2003;31(6):748–754.

18. Balevic SJ, Green TP, Clowse MEB, Eudy AM, Schanberg LE, Cohen-Wolkowicz M. Pharmacokinetics of hydroxychloroquine in pregnancies with rheumatic diseases. *Clin Pharmacokinet*. 2019;58(4):525–533.
19. Lim HS, Im JS, Cho JY, et al. Pharmacokinetics of hydroxychloroquine and its clinical implications in chemoprophylaxis against malaria caused by *Plasmodium vivax*. *Antimicrob Agents Chemother*. 2009;53(4):1468–1475.
20. Yao X, Ye F, Zhang M, et al. In vitro antiviral activity and projection of optimized dosing design of hydroxychloroquine for the treatment of severe acute respiratory syndrome coronavirus 2 (SARS-CoV-2). *Clin Infect Dis*. 2020. doi: 10.1093/cid/ciaa237. [Online ahead of print].
21. Wang W, Hallow KM, James DA. A Tutorial on RxODE: simulating differential equation pharmacometric models in R. *CPT Pharmacometrics Syst Pharmacol*. 2016;5(1):3–10.
22. European Medicines Agency (EMA). Summary on compassionate use: Remdesivir Gilead (Procedure No. EMEA/H/K/5622/CU). EMA web site. https://www.ema.europa.eu/en/documents/other/summary-compassionate-use-remdesivir-gilead_en.pdf. Published April 3, 2020. Accessed April 14, 2020.